

## Acrylamide Release Resulting from Sunlight Irradiation of Aqueous Polyacrylamide/Iron Mixtures

JAMES E. WOODROW,<sup>\*,†</sup> JAMES N. SEIBER,<sup>§</sup> AND GLENN C. MILLER<sup>†</sup>

Natural Resources and Environmental Science, University of Nevada, Reno, Nevada 89557, and  
 Agricultural Research Service, U.S. Department of Agriculture, Albany, California 94710

Linear anionic polyacrylamide (PAM) has been used in irrigation practices as a flocculating agent to minimize water losses through seepage in earthen canals. The stability of PAM is of concern because of the possibility of acrylamide (AMD) monomer release during environmental weathering. Aqueous solutions of commercial PAM mixed with ferric sulfate, subjected to simulated and natural sunlight irradiation, showed polymer chain scission and release of the AMD monomer. At acid/neutral pH, the amount of AMD released was directly related to the concentration of ferric ion and the irradiation time. At alkaline pH (~8), PAM/Fe<sup>3+</sup> mixtures were stable under irradiation. PAM chain scission involved the hydroxyl radical, but specific AMD release appeared to require PAM-bound iron. Low iron concentrations and alkaline pH of irrigation water would limit AMD release. Residual monomer in PAM can contribute AMD to irrigation water, but concentrations would remain below the U.S. EPA drinking water standard of 0.5 ppb.

**KEYWORDS:** Polyacrylamide; PAM; acrylamide; iron; sunlight

### INTRODUCTION

Commercial crystalline linear anionic polyacrylamide (PAM) is formed by the free radical induced polymerization of a mixture of acrylamide and acrylic acid/acrylate (1). The final dry product is a polymer that is capable of absorbing many times its mass of water by incorporating the water into the polymer structure through hydrogen bonding. When added to an excess of water, the polymer usually requires less than an hour to completely hydrate. In some irrigation practices, PAM is added directly to earthen canals as a flocculating agent to remove suspended sediment and, thereby, seal the canal and minimize seepage. An important concern with the use of PAM is its potential contribution of acrylamide (AMD) monomer to aquifers—some seepage will still occur—and to receiving waters (e.g., wetlands, recreational streams and lakes). Commercial PAM already contains a residual amount of AMD remaining from its production—usually <0.05% w/w. It has been known for some time that AMD is a suspect carcinogen and a cumulative neurotoxin (2). However, its health effects recently garnered worldwide attention and concern through a paper that described the formation of the monomer in cooked high-carbohydrate foods (3). Because of this paper, and others that followed, attention was also focused on other possible sources of AMD (e.g., irrigation practices) that could potentially affect human health.

There is little evidence in the literature that suggests AMD can be released when PAM is exposed to certain environmental

conditions. One study (4) claimed to have observed the slow release of AMD over several weeks from aqueous solutions of a polyacrylamide thickening agent (PAM mixed with an organic solvent) exposed to environmental sunlight conditions. Depending on the water source (natural surface and well water), AMD content increased by factors of 2–47 over a period of 2–5 weeks and then declined. Other investigators have questioned these results, their interpretation, and overall experimental design (5–7). Also, the results could not be replicated (6). Under the more extreme conditions of 254 nm UV light, aqueous solutions of PAM can release a small fraction of the AMD units (8). Another study observed a significant release of AMD from heated cross-linked polyacrylamide gels (9). However, no explanation for this was offered. The majority of studies to date in the literature have found that under environmental conditions of natural sunlight and/or ambient temperatures, oxidative conditions will commonly lead to chain scission, resulting in smaller molecular weight fragments of PAM but with no AMD release (7, 10–12).

In response to the concern over AMD in the environment, the U.S. Bureau of Reclamation (BOR) funded a two-year field and laboratory project to study the efficacy and stability of commercial PAM as a flocculating agent when applied to earthen irrigation canals and ditches. Our study was initiated, as part of the larger BOR project, to find and characterize the environmental conditions that might lead to AMD release and to relate the results to field use conditions. Many of the earlier studies concerned with PAM degradation had not considered how photocatalytic, complex-forming iron might affect the stability of the polymer. One exception was a study that examined the effect on PAM stability of added Fe<sup>2+</sup> in the absence of light, but monomer release was not observed,

\* Author to whom correspondence should be addressed [fax (775) 784-1142; e-mail jwoodrow@unr.nevada.edu].

† University of Nevada.

§ U.S. Department of Agriculture.

although polymer chain scission occurred (11). Another study looked at the photocatalytic degradation of PAM by  $\text{TiO}_2$  under 365 nm light (10), but this insoluble catalyst acted only as a source of hydroxyl radicals that attacked and degraded PAM, without any observed AMD enrichment. In this study, we exposed aqueous solutions of a commercial linear anionic PAM (the same product that was used in the BOR irrigation project) mixed with ferric sulfate to xenon-arc simulated sunlight and natural sunlight. Iron in the environment is more commonly found in this oxidation state. We selected iron because of its relative abundance, its common occurrence in natural waters, and its tendency toward redox cycling and free radical chemistry. Because surface water and groundwater can contain iron, the goal was to assess the stability of PAM under sunlight conditions with and without iron and, particularly, to look for evidence of AMD release.

## MATERIALS AND METHODS

**Preparation of Solutions.** Solutions for irradiation were prepared by combining 15 mL of the PAM [Tack Dry, Precision Polymer Corp., Greeley, CO; 70/30 amide/acrylate (sodium salt)] stock solution (~100 mg in 1000 mL) with various volumes of the ferric sulfate heptahydrate stock solution [10–11 mg in 100 mL (0.021–0.023 mg/mL  $\text{Fe}^{3+}$ )] and adding deionized (DI) water to a final volume of 100 mL, giving an approximate PAM concentration of 15 ppm in all cases. This concentration was the average of over 450 PAM assays of irrigation water samples taken during the BOR project. Enough ferric sulfate solution was added to a series of PAM solutions to achieve  $\text{Fe}^{3+}$  concentrations of 0.022, 0.215, 1.08, 2.24, 4.30, and 4.43 ppm (from  $\sim 4 \times 10^{-7}$  to  $\sim 8 \times 10^{-5}$  M).

Ethylenediaminetetraacetic acid (EDTA) stock solution (43–44 mg in 100–150 mL of DI water) was added to some PAM/ $\text{Fe}^{3+}$  (2 ppm) and  $\text{Fe}^{3+}$  (2 ppm) solutions (~17.5 ppm of EDTA). EDTA was used as a competing ligand to assess to what extent iron tended to bind to PAM and to assess the different effects of iron bound to EDTA and to PAM. Humic acid (HA) stock solution (10 mg in 100 mL of DI water) was added to some PAM solutions (10 ppm HA). HA, a common constituent of natural waters and a known source of reactive radical species, was included for comparison with iron.

**Measurement of pH.** A Brinkmann/Metrohm model 672 titroprocessor (Brinkmann Instruments, Westbury, NY) was used to measure the pH of each solution. All measurements were made in unbuffered solutions, because common buffers—acetate, phosphate, amine—interfered with the mechanism of the light/ $\text{Fe}^{3+}$ -catalyzed PAM decomposition, resulting in slower reaction rates. Instead, solution pH was adjusted using dilute solutions of hydrochloric acid and sodium hydroxide.

**Sunlight Irradiation.** Several 125 mL round Pyrex flasks with 24/40 standard taper ground-glass necks were filled with the 100 mL solutions and sealed with ground glass stoppers. The solutions were irradiated using a xenon-arc sunlight simulator equipped with a filter composed of coated glass with a cutoff at 290 nm (Hanau Suntest, DSET Laboratories, Phoenix, AZ). The simulator was able to closely approximate solar irradiance in the troposphere [equivalent to late summer noontime sunlight at 40° latitude (208  $\mu\text{W}/\text{cm}^2$  at 300 nm)]. Sample temperature was controlled to 30–31 °C by a fan inside the simulator. Separate flasks were irradiated for determination of PAM decline and AMD monomer release. For comparison, a few PAM/ $\text{Fe}^{3+}$  samples were placed outdoors on a building roof, where they were irradiated by summer sunlight for 1 day (July). Additional samples spiked with AMD standard, with and without added iron, remained outdoors during the summer for up to 30 days (July–August).

For PAM decline, the irradiated flasks were subsampled (~1 mL) every 15, 30, or 60 min for 3–8 h; longer sampling periods were used at lower  $\text{Fe}^{3+}$  concentrations. The 1 mL subsamples were sealed in 2 mL amber autosampler vials with crimped aluminum caps containing Teflon-lined butyl rubber septa (Agilent, Santa Clara, CA). The subsamples were assayed for PAM by HPLC (model 1100, Agilent)

using a 300 mm  $\times$  7.8 mm size exclusion TSK-GEL GMPWxl column (TOSOH Bioscience LLC, Montgomeryville, PA) and a diode array detector (DAD) set at 195 nm (10 nm bandwidth, 400 nm reference). The PAM was eluted using a 0.05 M aqueous monobasic potassium phosphate mobile phase at 0.8 mL/min and a column temperature of 45 °C. The instrument was calibrated using PAM standards in DI water (0.5–15.3 ppm) to generate six-point standard curves.

Additional samples were adjusted in pH to about 6 and 8 using dilute hydrochloric acid and sodium hydroxide. Irradiation and measurement of PAM decline were carried out as described above. As noted above, all samples were without added buffers. PAM itself showed some buffering capacity.

**Measurement of AMD Content.** After irradiation of PAM/ $\text{Fe}^{3+}$  mixtures for 3–8 h, 40 mL aliquots were removed and mixed, successively, with 7.5 g of potassium bromide, 0.5 mL of concentrated hydrobromic acid, and 2.5 mL of bromine-saturated water (Fisher Scientific, Fair Lawn, NJ) (13). The samples were mixed and stored in a cold refrigerator (0–4 °C) overnight (3). The samples were then removed from the refrigerator and allowed to warm to room temperature, and the excess bromine was eliminated by dropwise addition of 1 M aqueous sodium thiosulfate. To each sample was then added 15 g of sodium sulfate, followed by vigorous shaking to dissolve the salt, and the samples were extracted with  $2 \times 10$  mL of ethyl acetate (vigorous shaking for 2 min). The ethyl acetate extracts were separated from the aqueous solutions, dried with sodium sulfate (~1 g), transferred to 100 mL pear-shaped boiling flasks (Fisher Scientific), and reduced to about one-fourth of the original volume using a rotary evaporator under vacuum. The samples were then taken to dryness under a stream of dry nitrogen at atmospheric pressure. The residues were taken up into 0.25 mL of ethyl acetate and passed through 0.45  $\mu\text{m}$  membrane filters into 2 mL amber autosampler vials containing microliter glass inserts (Agilent). The vials were sealed with crimped aluminum caps containing Teflon-lined butyl rubber septa. Brominated AMD was assayed using gas chromatography–mass spectrometry (GC-MS; Agilent model 6890) with a 300 mm  $\times$  0.25 mm (i.d.) (0.25  $\mu\text{m}$  film) DB-5MS capillary column (J&W Scientific, Folsom, CA) and helium carrier at 1.4 mL/min. The GC column oven program was as follows: 60 °C (1 min hold), 10 °C/min to 190 °C (no hold), and 25 °C/min to 300 °C (2 min hold), giving a total run time of 20.4 min for each sample. The mass spectrometer was programmed to monitor for fragments *m/e* 106 and 108 ( $\text{C}_2\text{H}_3\text{Br}$ ) to account for the two isotopes of bromine. Initially, partial breakdown of brominated AMD occurred in the glass-lined GC injection port (250 °C), giving two peaks in the total ion chromatogram [ $\text{C}_2\text{H}_3\text{Br}$  and  $\text{C}_3\text{H}_4\text{BrNO}$  (*m/e* 149/151)]. A small plug of untreated glass wool was inserted into the glass liner in the injection port to promote complete conversion to a single peak ( $\text{C}_2\text{H}_3\text{Br}$ ). The analytical instrument was calibrated using brominated AMD standards (2,3-dibromopropionamide, 97%; Alfa Aesar, Pelham, NH) in ethyl acetate (0.06–1.00 ppm) to generate five-point standard curves.

For the sake of convenience, the single AMD-related brominated fragment ( $\text{C}_2\text{H}_3\text{Br}$ ) was used for routine assay of the monomer. However, for confirmation of AMD monomer release from PAM, the injection port glass wool was removed, allowing the formation of the amide fragment— $\text{C}_3\text{H}_4\text{BrNO}$ —in addition to the  $\text{C}_2\text{H}_3\text{Br}$  fragment.

**UV-Visible Spectrophotometry.** A recording spectrophotometer (UV-2401 PC; Shimadzu, Columbia, MD) was used to measure the absorbance of  $\text{Fe}^{3+}$ /EDTA solutions in the range of 250–450 nm. Measurements were made after the  $\text{Fe}^{3+}$ /EDTA solutions were allowed to equilibrate for several hours. Changes in absorbance of  $\text{Fe}^{3+}$ /EDTA solutions under xenon-arc irradiation were also measured.

## RESULTS AND DISCUSSION

**Sunlight Irradiation.** Figure 1 shows typical results for PAM/ $\text{Fe}^{3+}$  mixtures compared to PAM alone. For  $\text{Fe}^{3+}$  at about 2 ppm (pH ~6), the PAM decline half-life was about 3 h, compared to about 60 h for 0.02 ppm of  $\text{Fe}^{3+}$  (pH ~7.4). PAM alone showed a half-life of about 152 h (pH ~7.4). Duplicate PAM/ $\text{Fe}^{3+}$  (2 ppm) samples placed outdoors under summer sunlight for 1 day showed a PAM decline half-life of 3–4 h,

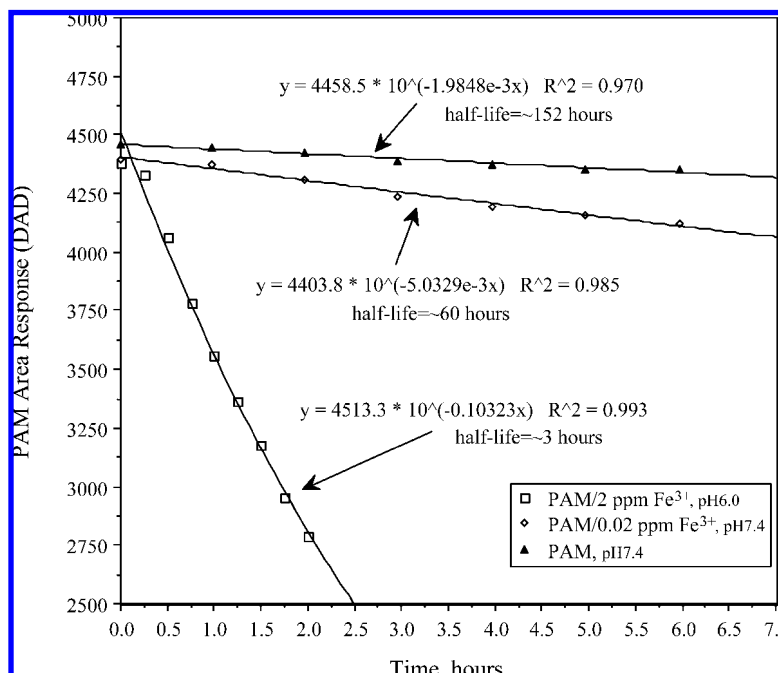


Figure 1. Decline of PAM alone and in the presence of  $\text{Fe}^{3+}$ .

which compared with 3 h in the laboratory photoreactor. Decline in PAM was due to polymer chain scission by a free radical mechanism involving hydroxyl radical (11, 12). With the size exclusion column, polymer chain scission was based on increasing retention time, which indicated decreasing average molecular weight for PAM. Retention times of the peak apex typically increased from about 7.5 min to over 12 min during the irradiation tests. This can be expressed in a Ln-linear relationship between elution volume (EV, product of flow rate and retention time) and polymer molecular weight (MW):

$$\text{EV} = -m \ln(\text{MW}) + b \quad (m = \text{slope}, b = \text{intercept})$$

This relationship means that the fraction of the polymer with the highest molecular weight will elute first (14). Because the HPLC instrument was not calibrated with standard polymers of known molecular weights, we cannot state unequivocally the extent of molecular weight reduction. However, other investigators using Fenton's reagent ( $\text{Fe}^{2+}$  plus hydrogen peroxide) have found that the addition of just 1 ppm of  $\text{Fe}^{2+}$  to a 50 ppm PAM solution resulted in a reduction of the PAM molecular weight by more than half (11). If we assume for our solutions that the PAM peak, from the beginning of the leading edge (6.5 min) to where the tail merged with the baseline (11.5 min), represents a typical molecular weight range of 24 million (6.5 min) to 12 million (11.5 min), then for the sunlight-irradiated PAM/ $\text{Fe}^{3+}$  samples we saw at least a 50% reduction in the average molecular weight ( $m = 5.771$ ,  $b = 103.266$  in the equation above). This was based on an observed shift of the peak apex to retention times of  $>12$  min (Figure 2). In our irradiation tests, PAM decline was also assessed through determination of the HPLC peak area response, which showed a decline over time. This indicated that some of the PAM fragments were small enough to be trapped by the inclusion volume of the pores of the analytical column.

Under the sunlight conditions of our study, the chemistry leading to decomposition of PAM was driven by solvated  $\text{Fe}^{3+}$  and  $\text{Fe}^{3+}$  complexed to PAM. In aqueous solution,  $\text{Fe}^{3+}$  forms ligand-to-metal charge-transfer complexes that can lead to

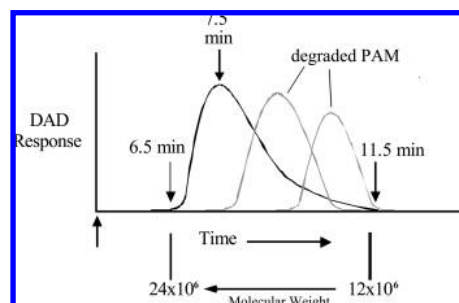
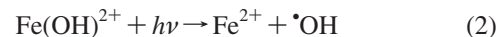


Figure 2. Liquid chromatograms of polyacrylamide showing typical shifts in retention times during sunlight irradiation ( $t_r = 7.5$  min for unexposed standard).

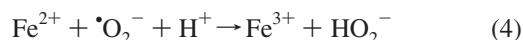
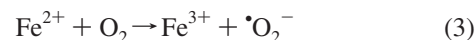
hydroxyl radical (15). For example,  $\text{Fe}^{3+}$  in solution will undergo hydrolysis:

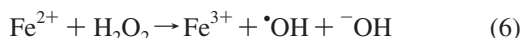
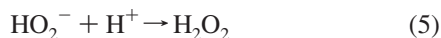


Then, in the presence of sunlight (omitting the extra waters of hydration), the hydrolyzed species will undergo photoreduction (16):



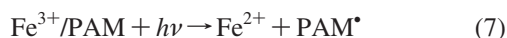
The  $\cdot\text{OH}$  radical can either back react with  $\text{Fe}^{2+}$  or react with PAM. Because  $\cdot\text{OH}$  reacts nonselectively and reactivity is effectively diffusion controlled, reaction with PAM will compete well with the back reaction because of its greater concentration in terms of the monomer unit density ( $[\text{PAM}] \approx 7 \times 10^{-10}$  M, equivalent to  $[\text{monomer}] \approx 2.0 \times 10^{-4}$  M (294,366 monomer units per mole of PAM);  $[\text{Fe}^{3+}] \approx 0.04\text{--}8.0 \times 10^{-5}$  M). Also, the reaction of  $\cdot\text{OH}$  with organics has a 1–2 orders of magnitude greater rate constant compared to its reaction with  $\text{Fe}^{2+}$  (15). The  $\text{Fe}^{2+}$  produced in reaction 2 can also autoxidize to generate more  $\cdot\text{OH}$  radical (reactions 3–6), as long as there is sufficient dissolved oxygen (12):



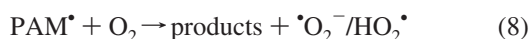


The last step is the well-known Fenton reaction. The ultimate production of the  $\cdot\text{OH}$  radical depends on the oxygen tension and reactions 3–6 will not occur if the solution is depleted of oxygen. However, oxygen depletion is not likely in flowing irrigation canals and ditches.

In addition to reactions 1 and 2, another source of  $\text{Fe}^{2+}$  would be the result of ligand-to-metal charge transfer for a  $\text{Fe}^{3+}$ /PAM complex:



This would lead to decomposition of PAM and the production of the superoxide free radical:



Hydroxyl radical would then be produced by reactions 4–6. The products of PAM decomposition, due to ligand-to-metal charge transfer and attack by hydroxyl radical, would include the monomer.

Autoxidation rate of  $\text{Fe}^{2+}$  is pH-dependent, as is the photoreduction rate of  $\text{Fe}^{3+}$ . For example, at pH 6 and 7, the half-lives for  $\text{Fe}^{2+}$  autoxidation are about 17 h and 10 min, respectively (12). This means that, on the basis of the stoichiometry of reaction 3 above, dissolved oxygen at alkaline pH would be depleted in nonaerated solutions—about 10 min at pH 7.4 (half-life = 1.6 min), compared to over 4.5 days at pH 6 for 99% consumption of dissolved oxygen (initial concentration of  $\sim 3 \times 10^{-4}$  M). By comparison,  $\text{Fe}(\text{OH})_2^{2+}$  photoreduction (reaction 2) at pH 6 and 7 will have approximate half-lives of 3 and >11.5 h, respectively (17). This means that, at acid pH,  $\text{Fe}^{2+}$  will accumulate relative to  $\text{Fe}^{3+}$ , whereas, at alkaline pH,  $\text{Fe}^{3+}$  will be the dominant species.

Because  $\text{Fe}^{2+}$  autoxidation and  $\text{Fe}^{3+}$  photoreduction are pH-dependent, solution pH had a dramatic effect on the rate of PAM decline in irradiated samples containing  $\text{Fe}^{3+}$ . For example, an  $\text{Fe}^{3+}$  solution of about 0.02 ppm had an initial pH of about 7.4 due to dissolved PAM. The pH was adjusted to 6.2 using dilute hydrochloric acid and then subjected to simulated sunlight irradiation, during which time the pH did not change significantly. Instead of a half-life of about 60 h, as illustrated in **Figure 1** (pH  $\sim 7.4$ ), the half-life at pH 6.2 was about 21 h, due to a faster  $\text{Fe}^{2+}$ /hydroxyl radical production rate at this pH. However, at pH 8, there was no observable change in PAM (i.e., no change in peak area and retention time) for a 2 ppm  $\text{Fe}^{3+}$  solution, whereas at pH 6 half-life for PAM was about 3 h, as shown in **Figure 1**. Other investigators have shown that iron redox cycling, starting with  $\text{Fe}^{3+}$  photoreduction, is not observed at pH 8 (17). Therefore,  $\text{Fe}^{2+}$  and hydroxyl radical were no longer being produced through the ligand-to-metal charge-transfer mechanism involving  $\text{Fe}^{3+}$ .

When EDTA was added to PAM/ $\text{Fe}^{3+}$  mixtures at 2 ppm of  $\text{Fe}^{3+}$ , the 3 h half-life was reduced to about 1–1.5 h, but with no increase in the amount of the AMD monomer released compared to PAM/ $\text{Fe}^{3+}$  mixtures alone. Other investigators have observed that small polycarboxylate ligands, when complexed with  $\text{Fe}^{3+}$ , show fairly rapid photolytic reactions ( $t_{1/2} \sim$  minutes) when irradiated with 436 nm light (18). These redox reactions were sources of  $\text{Fe}^{2+}$ ,  $\cdot\text{O}_2^-/\text{HO}_2\cdot$ ,  $\text{H}_2\text{O}_2$ , and, ultimately, hydroxyl radical. It is reasonable to assume that similar redox reactions would occur for an  $\text{Fe}^{3+}$ /EDTA complex. The absor-

bance spectrum of the complex in our test solutions showed maxima at 285–300 nm. Under simulated sunlight irradiation, the  $\text{Fe}^{3+}$ /EDTA complex will undergo a ligand-to-metal charge transfer leading to the formation of  $\text{Fe}^{2+}$  and to the decomposition of the complex—we observed a complete loss of the 285–300 nm absorbance after an hour of simulated sunlight irradiation in the absence of PAM. Estimated photolysis half-life for the complex was about 10 min, which compares with the results of other investigators (19–22). The  $\text{Fe}^{2+}$  would then undergo rapid autoxidation with the further production of hydroxyl radical, leading to accelerated PAM decline (reactions 3–6). An important decomposition step for EDTA is decarboxylation leading to carbon-centered radicals, which will give redox precursors to hydroxyl radical production. This is in line with the  $\text{Fe}^{3+}$ /polycarboxylate work of others (18). Therefore, the increased rate of PAM decline in the presence of  $\text{Fe}^{3+}$  and EDTA was due, for the most part, to increased production of hydroxyl radical because of the light-induced redox reactions of the  $\text{Fe}^{3+}$ /EDTA complex.

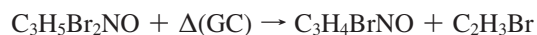
Humic acid (HA, 10 ppm) mixed with aqueous PAM resulted in a decline half-life of the polymer of about 41 h, compared to 152 h for irradiated PAM alone (**Figure 1**), but with no measurable release of the AMD monomer. HA is a photoreducing agent and, as such, can reduce dissolved oxygen to give hydrogen peroxide under sunlight irradiation. The hydrogen peroxide will react with organics, such as PAM, to ultimately produce hydroperoxy compounds that can generate reactive organic radicals in a series of complex reactions leading to decomposition of the polymeric material.

**AMD Content of Irradiated Samples.** The monomer alone in aqueous solution was relatively stable to photolysis. A 30 day exposure to natural sunlight yielded an approximate half-life of 100 days. In the presence of  $\text{Fe}^{3+}$ , AMD showed no measurable decline after 11 days of sunlight irradiation.

Only the PAM samples that contained  $\text{Fe}^{3+}$  showed evidence of AMD monomer release. **Table 1** and **Figure 3** summarize a comparison of AMD monomer concentrations with  $\text{Fe}^{3+}$  concentrations in 15 ppm PAM solutions, which initially contained almost immeasurable levels of AMD (<0.01 ppb). Compared to the results of other studies (4, 8, 9), AMD release in our study was rapid. It was clear that more  $\text{Fe}^{3+}$  resulted in more released monomer. For 2 ppm of  $\text{Fe}^{3+}$  in the outdoor samples under summer sunlight for 1 day (8 h), the AMD formation rate was 0.292 ppb/h, which compares well with the data in **Table 1**. Monomer release was confirmed by monitoring the occurrence of the amide fragment [ $\text{C}_3\text{H}_4\text{BrNO}$  ( $m/e$  149/151)] along with the  $\text{C}_2\text{H}_3\text{Br}$  fragment ( $m/e$  106/108) in the GC-MSD. That is, after AMD ( $\text{C}_3\text{H}_5\text{NO}$ ) bromination



decomposition of the brominated material in the GC injection port gave

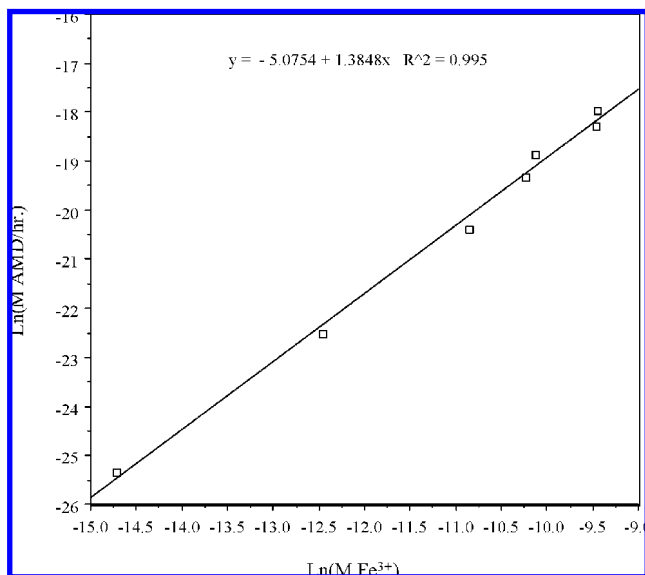


The latter was accomplished by removing the glass wool from the injection port of the instrument. **Figure 4** shows total ion chromatograms for a PAM blank (no AMD or  $\text{Fe}^{3+}$ ) (**A**), a PAM blank spiked with brominated AMD (no  $\text{Fe}^{3+}$ ) (**B**), and an irradiated PAM/ $\text{Fe}^{3+}$  sample (no added AMD) (**C**). The brominated ethene fragment ( $\text{C}_2\text{H}_3\text{Br}$ ) and amide fragment ( $\text{C}_3\text{H}_4\text{BrNO}$ ) had retention times of about 5.5 and 10.3 min, respectively.

Monomer release was the result of specific chain scission (unzipping) of the  $\text{Fe}^{3+}$ /PAM complex. Evidence for complex

**Table 1.** AMD Release versus Fe<sup>3+</sup> Concentrations for Xenon-Arc Irradiated PAM Solutions

| Fe <sup>3+</sup> , ppm | irrad time, h     | AMD, ppb          | AMD, ppb/h         |
|------------------------|-------------------|-------------------|--------------------|
| 4.43                   | 3.50              | 3.97              | 1.13               |
| 4.30                   | 3.08              | 2.52              | 0.818              |
| 2.24                   | 3.50              | 1.61              | 0.460              |
| 2.00 <sup>a</sup>      | 8.00 <sup>a</sup> | 2.34 <sup>a</sup> | 0.292 <sup>a</sup> |
| 1.08                   | 5.00              | 0.498             | 0.100              |
| 0.215                  | 5.00              | 0.059             | 0.012              |
| 0.022                  | 6.97              | 0.005             | 0.001              |

<sup>a</sup> Summer sunlight irradiation.**Figure 3.** AMD formation rate versus iron concentration.

formation between Fe<sup>3+</sup> and PAM was presented by other investigators who measured changes in viscosity of aqueous solutions upon the addition of Fe<sup>2+</sup>/Fe<sup>3+</sup>, which complexed with the amide groups (11, 23). When we added increasing amounts of Fe<sup>3+</sup> (0.026–5.10 ppm) to aqueous PAM solutions (15 ppm) in the absence of light, we observed an almost 10% shift to longer retention times for PAM on the HPLC size exclusion column. This resulted from a reduction in the hydrodynamic (gyratory) radius of the polymer due to complexation with Fe<sup>3+</sup> (24, 25). Furthermore, at relatively high Fe<sup>3+</sup> concentrations (>10 ppm), we observed the formation of a PAM/Fe<sup>3+</sup> flocculant. We did not observe this in our irradiated samples that had much lower Fe<sup>3+</sup> concentrations. For the latter, the PAM/Fe<sup>3+</sup> complex either remained in solution or existed as a colloidal suspension. Finally, when EDTA was added to a freshly prepared PAM/Fe<sup>3+</sup> solution, the resulting Fe<sup>3+</sup>/EDTA peak, using UV–vis spectrophotometry, had an absorbance that was 69% of that predicted by standard Fe<sup>3+</sup>/EDTA mixtures. When a PAM/Fe<sup>3+</sup> solution was allowed to remain overnight before the addition of EDTA, the absorbance of the resulting Fe<sup>3+</sup>/EDTA peak was only about 26% of that expected. The Fe<sup>3+</sup> not tied up by EDTA was bound to PAM. This is reasonable considering that the binding sites for the two ligands are the same—O and N (i.e., the binding energies were assumed to be similar for EDTA and PAM). All of these results suggest that Fe<sup>3+</sup> can easily bind to PAM, and the binding sites can serve as loci for monomer release under sunlight irradiation.

Ligand-to-metal charge transfer for the Fe<sup>3+</sup>/PAM complex could lead to carbon-centered radicals resulting in decomposition products, including the AMD monomer (18). This would ultimately lead to hydroxyl radical production where Fe<sup>3+</sup> is bound to PAM,

again affording an opportunity for monomer release. It is reasonable to assume that the acrylate monomer would be released as well, although the analytical method for AMD was not able to detect the acrylate. When EDTA was added early to our PAM/Fe<sup>3+</sup> mixtures, much of the Fe<sup>3+</sup> in solution was complexed by EDTA. Therefore, the rate of PAM decline was accelerated because of increased production of hydroxyl radical by the Fe<sup>3+</sup>/EDTA complex. However, the amount of AMD remained unchanged compared to PAM/Fe<sup>3+</sup> mixtures alone. These results compare with those from the irradiation of PAM/HA mixtures, in which PAM decline readily occurred because irradiated humic acid produced hydroxyl radicals, but no monomer release was observed, because Fe<sup>3+</sup> was not included.

Assuming an average molecular weight of about 20.9 million for PAM [derived from size exclusion HPLC of the pure polymer with a molecular weight range of 12–24 million (Figure 2)], PAM would contain about 206,000 moles of AMD per mole of PAM (70% amide, 30% acrylate). For the greatest enrichment from Table 1 (3.97 ppb), this means that only about 0.038% of the AMD units were converted to free AMD under the conditions of our study (i.e., ~380 AMD units per million amide units in the polymer). By contrast, the lowest AMD concentration (0.005 ppb) corresponded to about a  $5 \times 10^{-5}$ % release (0.5 AMD unit per million amide units). The data in Table 1 and Figure 3 imply that—at acid/neutral pH—there might not be a limit to the amount of AMD monomer released and that at higher Fe<sup>3+</sup> concentrations percent of AMD released could be even greater. Given that aqueous Fe<sup>3+</sup> photochemically/chemically cycles (reactions 1–8), AMD release should be continuous as long as sunlight and oxygen are available. Assays for iron in typical irrigation waters treated with PAM during the BOR project had concentrations on the order of 0.02 ppm and less (26). This means that, during the time needed for PAM to flocculate suspended material (usually less than an hour), on the order of about 10<sup>-5</sup>% AMD, at the most, would be released. This is based on an AMD release rate of 0.001 ppb/h (~1 × 10<sup>-11</sup> M/h) in the presence of 0.022 ppm of Fe<sup>3+</sup> (Table 1; Figure 3). This is much less than the residual AMD in commercial PAM (<0.05% w/w).

Under simulated and natural sunlight irradiation, PAM will rapidly undergo general chain scission into fragments, with and without Fe<sup>3+</sup>, as reflected in declining HPLC peak area response and average molecular weight. In the presence of Fe<sup>3+</sup>, a small fraction of this process (specific chain scission) will lead to release of monomer, as reflected in increasing AMD solution concentration with irradiation time and Fe<sup>3+</sup> concentration. A free radical mechanism, involving hydroxyl radical produced by ligand-to-metal charge transfer (Fe<sup>3+</sup>) and autoxidation (Fe<sup>2+</sup>), is responsible for the decomposition of PAM in aqueous solution at acid pH. However, PAM is relatively stable under alkaline conditions. Monomer release appears to be caused by Fe<sup>3+</sup> bound to PAM, where specific scission can take place. This was supported by tests with EDTA, which, when added to PAM/Fe<sup>3+</sup> mixtures, complexed with Fe<sup>3+</sup> and prevented further monomer release. Furthermore, a free radical mechanism alone will not release monomer, as shown by the irradiation results of a PAM/HA mixture. In the BOR field project, monomer release due to the photolysis of PAM-bound iron in irrigation water was not likely to be significant (<10<sup>-5</sup>%) because of the characteristically low iron concentrations (<0.02 ppm) and the alkaline pH (7.5–8.5). Any AMD in irrigation water resulting from the application of PAM was due to residual monomer remaining from the manufacture of the polymer (<0.05% w/w). Levels of the monomer in PAM-treated irrigation water—measured close to application points and up to several hundred

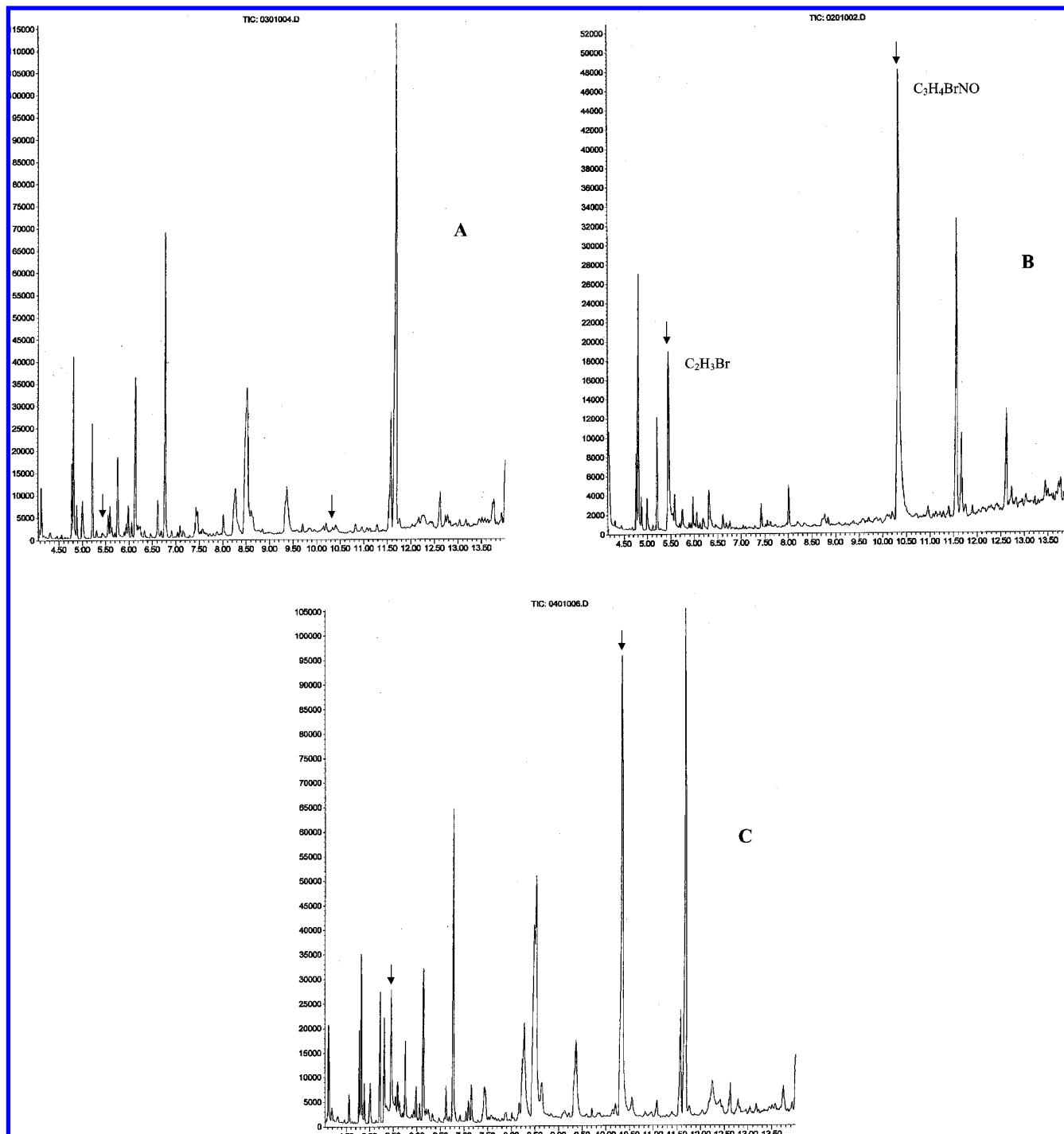


Figure 4. PAM blank (A), spiked PAM blank (B), and irradiated PAM/Fe<sup>3+</sup> mixture (C). Arrows indicate retention times for the peaks of interest.

meters downstream—were consistently less than the U.S. EPA drinking water standard of 0.5 ppb (27): 0.1–0.4 ppb (av = 0.2 ppb) (26). Of the 38 samples taken, only 16 had quantifiable AMD [ $\geq 0.1$  ppb (quantitation limit for irrigation water)], and they were the samples closest to the application points. The continuously flowing canal would further reduce the already low AMD levels.

#### SAFETY

Polyacrylamide has no known human health concerns. Acrylamide is a suspect carcinogen (category 2) and a cumulative neurotoxin. Because the vapor pressure of crystalline AMD is appreciable (0.9 Pa at 25 °C; 4.4 Pa at 40 °C), we worked with and stored the dry material in a fume hood away from sources of

heat. Organic and aqueous solutions were handled with safety outside a fume hood because of the monomer's high solubility in most solvents.

#### ACKNOWLEDGMENT

We acknowledge the technical assistance of Sandra Carroll and Veronica Edirveerasingam.

#### LITERATURE CITED

- (1) Caulfield, M. J.; Qiao, G. G.; Solomon, D. H. Some aspects of the properties and degradation of polyacrylamides. *Chem. Rev.* **2002**, *102*, 3067–3083.

- (2) *Acrylamide—European Union Risk Assessment Report*; Hansen, B. G., Munn, S. J., Luotamo, M., Musset, C. de Bruijn, J., Pakalin, S., Berthault, F., Vegro, S.; Pellegrini, G., Allanou, R., Scheer, S., Eds.; Office for Official Publications of the European Communities: Luxembourg, 2002; Vol. 24, 207 pp.
- (3) Tareke, E.; Rydberg, P.; Karlsson, P.; Eriksson, S.; Törnqvist, M. Analysis of acrylamide, a carcinogen formed in heated foodstuffs. *J. Agric. Food Chem.* **2002**, *50*, 4998–5006.
- (4) Smith, E. A.; Prues, S. L.; Oehme, F. W. Environmental degradation of polyacrylamides. II. Effects of environmental (outdoor) exposure. *Ecotoxicol. Environ. Saf.* **1997**, *37*, 76–91.
- (5) Kay-Shoemake, J. L.; Watwood, M. E.; Lentz, R. D.; Sojka, R. E. Polyacrylamide as an organic nitrogen source for soil microorganisms with potential effects on inorganic soil nitrogen in agricultural soil. *Soil Biol. Biochem.* **1998**, *30*, 1045–1052.
- (6) Ver Vers, L. M. Determination of acrylamide monomer in polyacrylamide degradation studies by high-performance liquid chromatography. *J. Chromatogr. Sci.* **1999**, *37*, 486–494.
- (7) Gao, J.; Lin, T.; Wang, W.; Yu, J.; Yuan, S.; Wang, S. Accelerated chemical degradation of polyacrylamide. *Macromol. Symp.* **1999**, *144*, 179–185.
- (8) Caulfield, M. J.; Hao, X.; Qiao, G. G.; Solomon, D. H. Degradation of polyacrylamides. Part I. Linear polyacrylamide. *Polymer* **2003**, *44*, 1331–1337.
- (9) Holliman, P. J.; Clark, J. A.; Williamson, J. C.; Jones, D. L. Model and field studies of the degradation of cross-linked polyacrylamide gels used during the revegetation of slate waste. *Sci. Total Environ.* **2005**, *336*, 13–24.
- (10) Vijayalakshmi, S. P.; Madras, G. Photocatalytic degradation of poly(ethylene oxide) and polyacrylamide. *J. Appl. Polym. Sci.* **2006**, *100*, 3997–4003.
- (11) Ramsden, D. K.; McKay, K. Degradation of polyacrylamide in aqueous solution induced by chemically generated hydroxyl radicals: Part I—Fenton's reagent. *Polym. Degrad. Stab.* **1986**, *14*, 217–229.
- (12) Ramsden, D. K.; McKay, K. The degradation of polyacrylamide in aqueous solution induced by chemically generated hydroxyl radicals: Part II—autoxidation of Fe<sup>2+</sup>. *Polym. Degrad. Stab.* **1986**, *15*, 15–31.
- (13) U.S. Environmental Protection Agency. Acrylamide by gas chromatography, Method 8032A, 1996.
- (14) Kato, Y.; Matsuda, T.; Hashimoto, T. New gel permeation column for the separation of water-soluble polymers. *J. Chromatogr.* **1985**, *332*, 39–46.
- (15) Larson, R. A.; Schlauch, M. B.; Marley, K. A. Ferric ion promoted photodecomposition of triazines. *J. Agric. Food Chem.* **1991**, *39*, 2057–2062.
- (16) Langford, C. H.; Carey, J. H. The charge transfer photochemistry of the hexaquoiron(III) ion, the chloropentaaquoiron(III) ion, and the *m*-dihydroxo dimer explored with tert-butyl alcohol scavenging. *Can. J. Chem.* **1975**, *53*, 2430–2435.
- (17) King, D. W.; Aldrich, R. A.; Charnock, S. E. Photochemical redox cycling of iron in NaCl solutions. *Mar. Chem.* **1993**, *44*, 105–120.
- (18) Faust, B. C.; Zepp, R. G. Photochemistry of aqueous iron(III)–polycarboxylate complexes: Roles in the chemistry of atmospheric and surface waters. *Environ. Sci. Technol.* **1993**, *27*, 2517–2522.
- (19) Svenson, A.; Kaj, L.; Björndal, H. Aqueous photolysis of the iron (III) complexes of NTA, EDTA and DTPA. *Chemosphere* **1989**, *18*, 1805–1808.
- (20) Frank, R.; Rau, H. Photochemical transformation in aqueous solution and possible environmental fate of ethylenediaminetetraacetic acid (EDTA). *Ecotoxicol. Environ. Saf.* **1990**, *19*, 55–63.
- (21) Kari, F. G.; Hilger, S.; Canonica, S. Determination of the reaction quantum yield for the photochemical degradation of Fe(III)-EDTA: Implications for the environmental fate of EDTA in surface waters. *Environ. Sci. Technol.* **1995**, *29*, 1008–1017.
- (22) Laan, R. G. W.; Verburg, T.; Wolterbeek, H. T.; de Goeij, J. J. M. Photodegradation of iron(III)-EDTA: Iron speciation and domino effects on cobalt availability. *Environ. Chem.* **2004**, *1*, 107–115.
- (23) Yen, H.-Y.; Yang, M.-H. The effect of metal ions additives on the rheological behavior of polyacrylamide solution. *Polym. Testing* **2003**, *22*, 389–393.
- (24) Muller, G.; Laine, J. P.; Fenyó, J. C. High-molecular-weight hydrolyzed polyacrylamides. I. Characterization. Effect of salts on the conformational properties. *J. Polym. Sci.* **1979**, *17*, 659–672.
- (25) Lu, J. H.; Wu, L.; Letey, J. Effects of soil and water properties on anionic polyacrylamide sorption. *Soil Sci. Soc. Am. J.* **2002**, *66*, 578–584.
- (26) Susfalk, R. B.; Sada, D.; Martin, C.; Young, M. H.; Gates, T.; Rosamond, C.; Fitzgerald, B.; Mihevc, T.; Arrowood, T.; Shanfield, M.; Epstein, B.; Lutz, A.; Woodrow, J.; Miller, G.; Smith, D. M. *Field Application of Granular Linear Anionic Polyacrylamide (LA-PAM) to Water Delivery Canals for Water Conservation*; Desert Research Institute, Division of Hydrologic Sciences: Reno, NV, 2008.
- (27) U.S. Environmental Protection Agency, www.epa.gov/safewater.

Received for review December 17, 2007. Revised manuscript received February 11, 2008. Accepted February 12, 2008. This study was supported by the U.S. Bureau of Reclamation (Award 06-FC-81-1245).

JF703677V